Solar Energy Materials & Solar Cells 94 (2010) 2108–2112

Contents lists available at ScienceDirect

Solar Energy Materials & Solar Cells

journal homepage: www.elsevier.com/locate/solmat

Analysis of multi-crystalline silicon solar cells at low illumination levels using a modified two-diode model

A. Kassis *, M. Saad

Atomic Energy Commission of Syria, P.O. Box 6091, Damascus, Syria

ARTICLE INFO

Article history:
Received 12 April 2010
Received in revised form
22 June 2010
Accepted 25 June 2010

Keywords:
Multi-crystalline silicon
Two-diode model
Recombination
Grain boundaries
Low illumination

ABSTRACT

Current–voltage characteristics of multi-crystalline silicon solar cells measured under several low illumination levels are analyzed. The fitting analysis is conducted using a modified two-diode equivalent circuit accounting for an additional ohmic series resistance in the vicinity of grain boundaries and allowing for variable diode ideality factors. Apart from the shunt resistance—a key factor at very low illumination levels—the model indicates two other current transport mechanisms at low illumination levels, both related to recombination, but each of them can be allocated to a different region in the cell: (1) recombination in the crystalline region and (2) recombination at grain boundaries. The role played by each mechanism is studied depending on illumination level.

1. Introduction

Multi-crystalline silicon solar cells constitute one of the main solar cell branches on the PV market; still, there is room for enhancing the efficiency of these cells in comparison with mono-crystalline ones. Losses in multi-crystalline cells are often put in relation with grain boundaries, where recombination is likely to take place. Therefore, current transport in these cells is better described through a model that takes the effect of grain boundaries into consideration. Increasingly, the one-diode model usually applied to analyze *I–V* characteristics of multi-crystalline silicon solar cells is making way for different forms of the two-diode model [1–4], especially at low illumination levels [2]. This is the case when solar cells are utilized for indoor applications. Some groups even proposed a 3-diode equivalent circuit, accounting for a large leakage current through periphery [5].

Having decided in favor of a two-diode model, it is important to identify the current transport mechanism of each diode and its domain of action in the cell. Most groups proposing two-diode models for describing current transport in multi-crystalline silicon solar cells use constant diode ideality factors $n_1=1$ and $n_2=2$ [4–8]. This would mean that the first mechanism is an ideal diffusion one and the second mechanism is recombination at defects with an energy level exactly equal to the intrinsic Fermi level (i.e. with an activation energy exactly equal to half the energy gap of the absorber). Although the assumption of constant diode ideality factors would simplify the fitting analysis by reducing the number of fitting parameters, it represents a strong restriction of the possible current transport mechanisms that may result from the analysis and of the possible activation energies of the transport mechanisms.

On the other hand and in order to identify the contribution of each mechanism to the whole cell performance, a method was presented recently [9], which calculates the fraction of photo-current needed to compensate for the loss current of each mechanism under open circuit condition. The so calculated compensation current in each branch of the equivalent circuit is a measure of the role played by the corresponding mechanism in limiting cell performance.

In this paper, a modified two-diode model is presented that accounts for an additional ohmic series resistance in the vicinity of grain boundaries and assumes variable diode ideality factors—representing the reality more accurately. The application of the model is carried out on *I–V* characteristics of multi-crystalline silicon solar cells at room temperature and under various low illumination levels. Furthermore, the compensation current in each branch of the equivalent circuit is deduced depending on illumination level.

2. The model

Our model is a modified two-diode equivalent circuit (see Fig. 1) based on the following assumptions:

- The cell consists of two different regions with different current transport mechanisms: the crystalline region and the grain

* Corresponding author. Tel.: +963 11 2132580; fax.: +963 11 6112289.
E-mail address: pscientific2@aec.org.sy (A. Kassis).

0927-0248/$ - see front matter © 2010 Elsevier B.V. All rights reserved.
doi:10.1016/j.solmat.2010.06.036

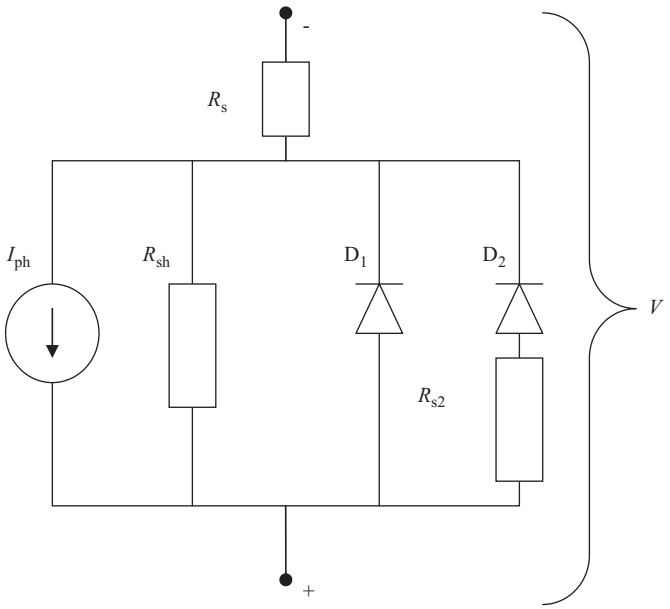

Fig. 1. Modified two-diode equivalent circuit used in this study for analyzing the multi-crystalline silicon solar cell.

boundary region, accounted by the two parallel diodes D_1 and D_2 in the equivalent circuit, respectively.

- The grain boundary region exhibits an additional series resistance since the resistivity in the vicinity of grain boundaries is higher than that within the crystallites [10]. This is accounted for by R_{s2}, which is connected to D_2 in Fig. 1.
- A shunt resistance R_{sh} is connected in parallel to both diodes D_1 and D_2. Furthermore, a series resistance R_s is connected to all three branches.
- The equations describing current transport through the cell contain variable diode ideality factors, so that the restriction of current transport mechanisms mentioned above is lifted.

In accordance with this equivalent circuit, the total current that flows through the cell can be written as follows:

$$I(V) = I_1(V) + I_2(V) + \frac{[V - I(V)R_s]}{R_{sh}} + I_{ph} \quad (1)$$

Here R_s is the series resistance, R_{sh} the shunt resistance and I_{ph} the photo-current. The quantities $I_1(V)$ and $I_2(V)$ represent currents that flow through diode D_1 and diode D_2, respectively, and can be written as

$$I_1(V) = I_{01}\left\{\exp\left[\frac{q[V - I(V)R_s]}{n_1 kT}\right] - 1\right\} \quad (2)$$

$$I_2(V) = I_{02}\left\{\exp\left[\frac{q[V - I(V)R_s - I_2(V)R_{s2}]}{n_2 kT}\right] - 1\right\} \quad (3)$$

where I_{01} and I_{02} are the saturation currents, n_1 and n_2 the diode ideality factors, q is the electron charge, k the Boltzmann constant, T the absolute temperature and R_{s2} is an additional series resistance connected to D_2.

3. Experimental

The analyzed cell was a 7.7 cm^2 partition of a cell denoted Q6-1380 (not encapsulated), which was thankfully provided by Q-Cells AG, Germany. Table 1 summarizes the cell properties taken from its data sheet. Current–voltage characteristics of the analyzed cell were measured at room temperature and investigated under several low illumination levels. Measurements were performed using a Keithley 238 Source Measure Unit (SMU) through a four-point connection. Halogen lamps were used for illumination, whereas a silicon calibration cell was used to set the illumination level. The illumination level was varied between 0 mW/cm^2 (dark) and 20 mW/cm^2. Fig. 2 presents the illumination level dependent I–V characteristics performed at room temperature.

Table 1
Data of the cell Q6-1380 provided by Q-Cells AG, Germany. The analyzed cell was a 7.7 cm^2 partition of this cell.

Product	Multi-crystalline silicon solar cell
Format	150×150 $mm^2 \pm 1$ mm
Thickness	300 μm ± 40 μm
Front (−)	2 mm bus bars (silver), blue anti-reflection coating (silicon nitride)
Back (+)	5 mm wide soldering pads (silver/aluminum), back surface field (aluminum)

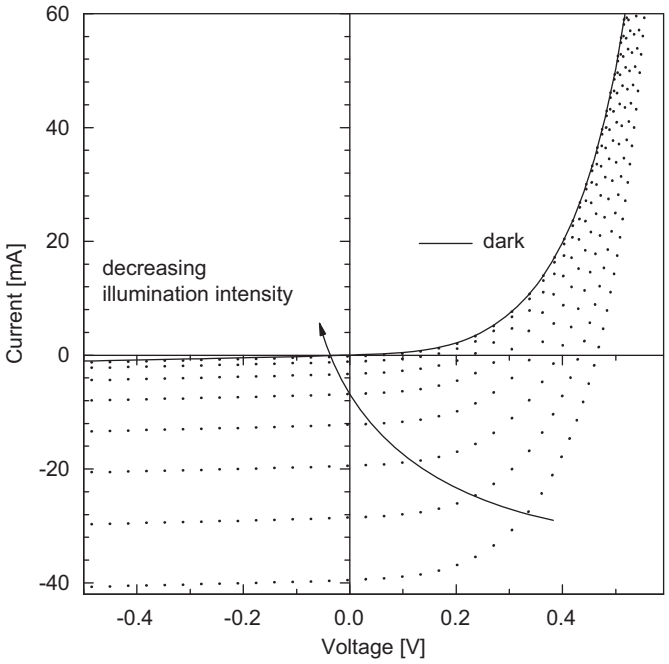

Fig. 2. Illumination-level-dependent current–voltage characteristics for the analyzed solar cell performed at room temperature.

4. Analysis and discussion

Current–voltage fitting characteristics of a multi-crystalline silicon solar cell were analyzed using the model presented above. The fitting method used was a least squares method. The need for a two-diode model for describing this cell is demonstrated through a comparison between the fitting results of its dark I–V curve, first with an one-diode model (deleting the branch of D_2 and R_{s2} in Fig. 1), and then with the two-diode model proposed above (Fig. 1). Table 2 shows the fitting parameters in each case, where it is clear that the two-diode fit gives a better χ^2 value than the one-diode fit by two orders of magnitude. Furthermore, Fig. 3 presents a comparison between the two fits, showing the need for the two-diode fit especially in the voltage region between 0.2 and 0.5 V.

Table 3 summarizes the parameters obtained by analyzing the I–V characteristics measured at room temperature under several illumination levels.

Table 2
Comparison between the parameters obtained from fitting the measured dark *I–V* characteristic of the studied cell using first a one-diode model, and then the two-diode model proposed.

	R_{sh} (Ω)	R_{s2} (Ω)	R_s (Ω)	n_2	I_{02} (A)	n_1	I_{01} (A)	χ^2 (A^2)
One-diode model	569.6		0.0413			3.236	1.243E−4	2.83E−4
Two-diode model	568.3	1.6425	0.1645	2.949	1.491E−4	1.411	1.117E−8	6.23E−7

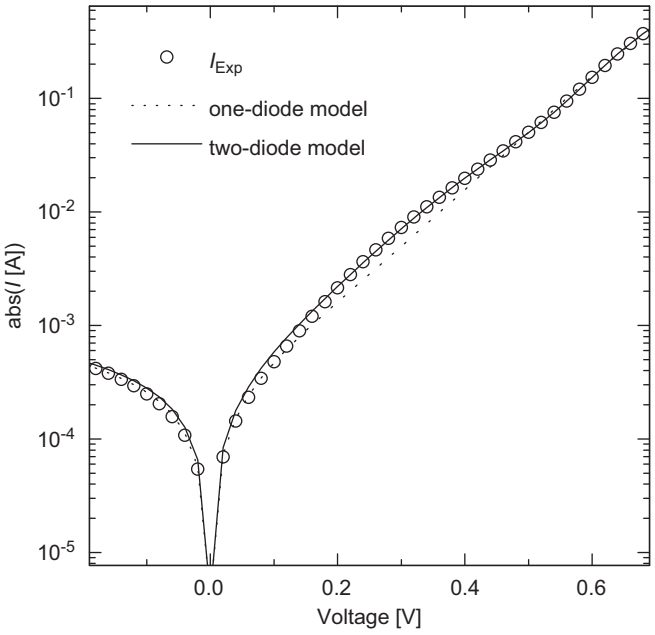

Fig. 3. Comparison between two fits of the dark *I–V* characteristic using first a one-diode model, and then the two-diode model proposed. The discrepancy is largest in the range between 0.2 and 0.5 V.

Since the model allocates D_1 to the crystalline region and D_2 (with the additional series resistance R_{s2}) to the grain boundary region, it is obvious that parameter set (I_{01}, n_1) describes current transport in the crystalline region, while parameter set (I_{02}, n_2) characterizes current passing along grain boundaries. In the following, a closer investigation of the obtained ideality factor values is presented.

In the literature, a value of n between 1 and 2 is often interpreted in terms of the Shockley–Read–Hall (SRH) model [11,12]. According to this model, the diode ideality factor should be equal to 2 if recombination in the space charge region (SCR) takes place via a single trap level in the middle of the absorber band gap; however, for an exponential distribution of trap states in the SCR and depending on the doping concentrations and energetic and spatial distribution of the recombination centers, the value of n may vary between 1 and 2 [13–15]. Another possible interpretation for diode ideality factor values between 1 and 2 is that current is dominated by a combination between recombination in the SCR and recombination in the (neutral or quasi-neutral) bulk [16]. In many cases, describing the cell with a single diode model reveals a diode ideality factor between 1 and 2 (interpreted as a combination of both diffusion as well as recombination in the SCR at the same time [17]); however, describing the same cell with the double-diode model would reveal the standard values of $n_1=1$ and $n_2=2$, which is then interpreted as diffusion for the first diode and recombination for the second [4]. In this paper, the values of n_1 (for diode D_1) lie between $n_1=1.36$ and $n_1=1.41$. This indicates that current transport in the crystalline region of the studied cell is controlled either by recombination in the SCR at an exponential distribution of trap states in the absorber band gap or by recombination in both SCR and bulk (quasi-neutral region) or by both diffusion as well as recombination in the SCR. The term "recombination in the crystalline region" (as opposed to the grain boundary region) is found suitable for describing these possibilities here.

A diode ideality factor greater than 2, although rarely presented for laboratory crystalline silicon cells, is often observed for industrial cells [18]. Generally, such relatively large diode ideality factors are observed in hetero-junction devices (e.g. solar cells based on chalcopyrite compounds); these factors are thought to result from recombination at a high density of defect states, either directly [19–21] or assisted by tunneling [22–24]. In polycrystalline silicon, high density of electrically active defect states is likely to be found at grain boundaries [25,26]. In this paper, the values of n_2 (for diode D_2) lie between $n_2=2.95$ and $n_2=3.1$. This indicates that current transport in the grain boundary region of the studied cell is controlled by recombination at a high density of defect states in this region.

Furthermore, Table 3 clearly shows that illumination of the cell does not lead to large changes in diode parameters (with the exception of the photo-current I_{ph}). This is in line with the relatively ideal behavior of silicon solar cells concerning their stability under illumination. Nevertheless, there is a slight decrease in the parameters of D_1 (I_{01}, n_1), which could be attributed to a deactivation of recombination defects in the gap by light irradiance through the higher quasi-Fermi level under light. This slight decrease in diode parameters was also found for some thin film Cu(In,Ga)Se_2 cells [27]. On the other hand, there is a slight increase in the parameters of D_2 (I_{02}, n_2) with increasing illumination level, which could be attributed to an increase in number of effective grain boundary recombination defects in a similar manner to interface recombination presented earlier [19]. It is worth mentioning that the change in diode parameters of D_2 (I_{02}, n_2) due to illumination is far less than the change found for the $CuGaSe_2$ cell presented in Refs. [20,22]. Moreover, values of R_{s2} are approximately an order of magnitude higher than those of R_s, in line with the higher resistivity at grain boundaries [10].

Furthermore, the method presented in Ref. [9] is used to calculate the fraction of photo-current needed to compensate for the loss current of each mechanism under open circuit condition. Fig. 4 shows the equivalent circuit for the cell under open circuit condition, where I_{c1}, I_{c2} and I_{c3} are the compensation currents in the three branches, whose sum equals the cell photo-current (I_{ph} in Fig. 1).

Table 4 summarizes the calculated compensation currents I_{c1}, I_{c2} and I_{c3} for the three branches in Fig. 4 depending on illumination level. The last column in Table 4 contains the value of the ratio of recombination current to cell photo-current $r=I_{c2}/I_{ph}$. This parameter is practically the same as the parameter denoted also as r in Ref. [4]. There, it represented the ratio of recombination area to the whole cell area and was considered a fitting parameter. It is worth mentioning that applying the separation method presented in Ref. [9] would lead to a reduction in the number of fitting parameters by one without losing any information.

Table 3
Diode parameters of the analyzed multi-crystalline silicon solar cell determined for different illumination levels using Eq. (1). The quantities I_{ill}, I_{ph}, n_1, n_2, I_{01}, I_{02}, R_s and R_{sh} represent illumination level, photo-current, diode ideality factors of D_1 and D_2, saturation currents of D_1 and D_2, series resistance and shunt resistance, respectively. R_{s2} is an additional series resistance connected to D_2.

I_{ill} (mW/cm^2)	R_{sh} (Ω)	R_{s2} (Ω)	R_s (Ω)	n_2	I_{02} (A)	n_1	I_{01} (A)	I_{ph} (A)
20	471.9	1.386	0.173	3.096	1.866E−4	1.361	6.473E−9	3.949E−2
14.5	510.6	1.462	0.170	3.065	1.806E−4	1.376	7.695−9	2.859E−2
9.84	481.8	1.493	0.168	3.034	1.716E−4	1.384	8.370E−9	1.942E−2
6.20	500.5	1.582	0.167	2.999	1.660E−4	1.395	9.479E−9	1.225E−2
3.47	501.6	1.603	0.167	2.975	1.592E−4	1.340	9.879E−9	6.844E−3
1.66	516.4	1.626	0.166	2.968	1.572E−4	1.405	1.049E−8	3.283E−3
0.58	530.5	1.643	0.166	2.958	1.540E−4	1.409	1.090E−8	1.144E−3
0.10	543.5	1.652	0.166	2.949	1.512E−4	1.410	1.107E−8	2.045E−4
0 (dark)	568.3	1.643	0.165	2.949	1.491E−4	1.411	1.117E−8	0

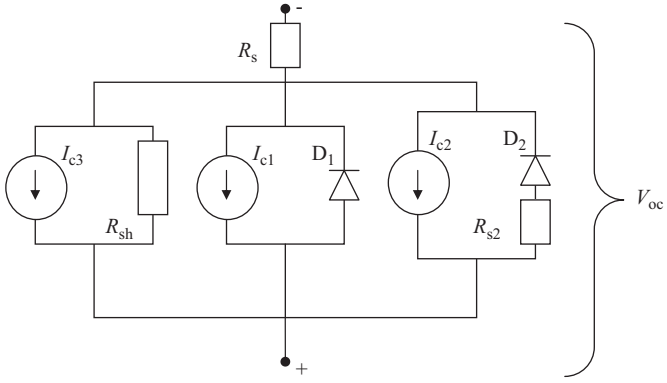

Fig. 4. Modified two-diode equivalent circuit under open circuit condition. I_{c1}, I_{c2} and I_{c3} are the compensation currents in the three branches, whose sum equals the cell photo-current (I_{ph} in Fig. 1).

Table 4
Calculated compensation currents I_{c1}, I_{c2} and I_{c3} for the three branches in Fig. 4 depending on illumination level I_{ill}. The quantity I_{ph} is cell photo-current and r is the recombination current ratio.

I_{ill} (mW/cm^2)	I_{ph} (A)	I_{c1} (A)	I_{c2} (A)	I_{c3} (A)	$r=I_{c2}/I_{ph}$
20	3.949E−2	3.67E−3	3.47E−2	9.96E−4	0.88
14.5	2.859E−2	1.62E−3	2.64E−2	8.48E−4	0.92
9.84	1.942E−2	5.38E−4	1.82E−2	8.20E−4	0.94
6.20	1.225E−2	1.34E−4	1.14E−2	6.85E−4	0.93
3.47	6.844E−3	5.39E−5	6.22E−3	5.88E−4	0.91
1.66	3.283E−3	4.20E−6	2.83E−3	4.31E−4	0.86
0.58	1.144E−3	6.91E−7	8.70E−4	2.65E−4	0.76
0.10	2.045E−4	6.40E−8	1.05E−4	8.10E−5	0.51

For a better illustration, the three compensation currents I_{c1}, I_{c2} and I_{c3} are presented in Fig. 5 versus cell photo-current. It is readily seen in this figure that while I_{c2} remains of the same order of magnitude as I_{ph} over the range of 3 decades, I_{c1} goes through 5 orders of magnitude and remains always below I_{c2} in that range. The value of I_{c3} indicates the beginning of a saturation behavior, and even a linear fit of I_{c3} shows that at standard illumination level only a small fraction of I_{ph} is needed to compensate for the cell shunt current. On the other hand, extrapolating the behavior of I_{c1} and I_{c2} to standard illumination level (as seen in Fig. 5) would result in I_{c1} and I_{c2} being of the same order of magnitude. This would be in accordance with what was found in Ref. [4], namely, the value of r between 0.35 and 0.74, meaning that diffusion current and recombination current are of the same order of magnitude. From Table 4, it is also clear that at very low illumination levels the main competition to compensate for the generated photo-current is between recombination current in the

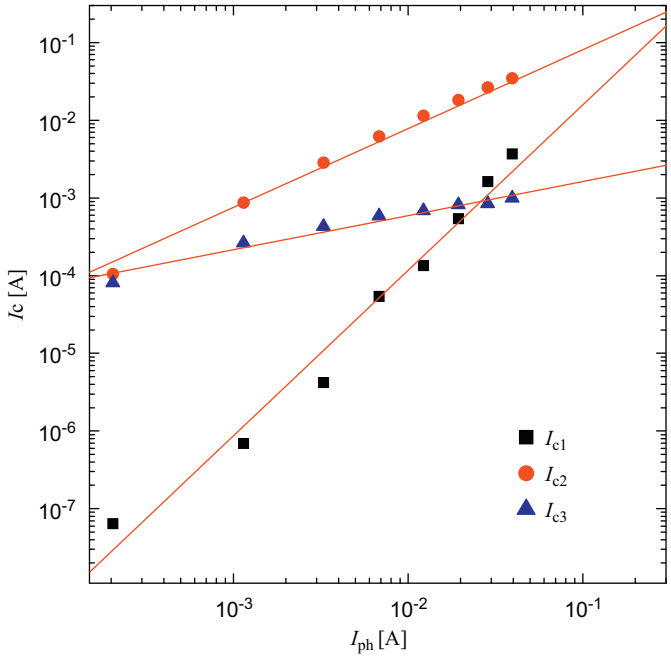

Fig. 5. Compensation currents I_{c1}, I_{c2} and I_{c3} versus cell photo-current I_{ph}. Linear best fits are also drawn for all three curves. At standard illumination level (at which $I_{ph} \approx 0.2$ A for the studied cell) I_{c3} remains relatively small, while I_{c1} and I_{c2} become of the same order of magnitude.

grain boundary region and shunt current, while at higher levels the competition is mainly between recombination at grain boundaries and recombination within crystallites.

From the parameters (I_0 and n) of each diode, it can be stated that diode D_1 is more favorable to good cell performance than diode D_2. Assigning the first mechanism to the crystalline region and the second one to the grain boundary region makes it straightforwardly understandable that an enlargement of crystallite size will directly enhance cell performance [28].

5. Conclusion

A modified two-diode equivalent circuit accounting for an additional ohmic series resistance in the vicinity of grain boundaries was proposed in order to accurately describe current–voltage characteristics of multi-crystalline silicon solar cells, especially under low illumination levels. The model allows for variable ideality factors, resulting in a more precise insight into current transport mechanisms. Two mechanisms were found to dominate current transport at low illumination levels: recombination in the crystalline region and recombination at

grain boundaries. At very low illumination levels, the main competition to compensate for the generated photo-current is between shunt current and recombination current in the grain boundary region. Furthermore, the clear assignment of one branch of the equivalent circuit to the grain boundary region enables the evaluation of the influence of grain boundaries on solar cell performance.

References

[1] M. Wolf, G.T. Noel, R.J. Strin, Investigation of the double exponential in the current voltage characteristics of silicon solar cells, IEEE Trans. Electron Devices 24 (1977) 419–428.

[2] D.S.H. Chan, J.C.H. Phang, Analytical methods for the extraction of solar cell single- and double-diode model parameters from *I–V* characteristics, IEEE Trans. Electron Devices 34 (1987) 286–293.

[3] U. Stutenbaeumer, B. Mesfin, Equivalent model of monocrystalline, polycrystalline and amorphous silicon solar cells, Renewable Energy 18 (1999) 501–512.

[4] K. Kurobe, H. Matsunami, New two-diode model for detailed analysis of multicrystalline silicon solar cells, Jpn. J. Appl. Phys. 44 (2005) 8314–8321.

[5] K. Nishioka, N. Sakitani, Y. Uraoka, T. Fuyuki, Analysis of multicrystalline silicon solar cells by modified 3-diode equivalent circuit model taking leakage current through periphery into consideration, Sol. Energy Mater. Sol. Cells 91 (2007) 1222–1227.

[6] J.M. Zhu, W.Z. Shen, Y.H. Zhang, H.F.W. Dekkers, Determination of effective diffusion length and saturation current density in silicon solar cells, Physica B 335 (2005) 408–416.

[7] K. Taretto, U. Rau, J.H. Werner, Method to extract diffusion length from solar cell parameters—application to polycrystalline silicon, J. Appl. Phys. 93 (9) (2003) 5447–5455.

[8] D. Kray, S. Hopman, A. Spiegel, B. Richerzhagen, G.P. Willeke, Study on the edge isolation of industrial silicon solar cells with waterjet-guided laser, Sol. Energy Mater. Sol. Cells 91 (2007) 1638–1644.

[9] A. Kassis, M. Saad, Separation of solar cell current into its constituent parallel currents under illumination, Renewable Energy 34 (2009) 965–969.

[10] S.E. Lee, D.G. Lim, J. Yi, Novel type of multicrystalline silicon solar cell with an additional electrode along the grain boundaries, J. Korean Phys. Soc. 37 (1) (2000) 64–68.

[11] W. Shockley, W.T. Read, Statistics of the recombination of holes and electrons, Phys. Rev. 87 (5) (1952) 835–848.

[12] R.N. Hall, Electron–hole recombination in germanium, Phys. Rev. 87 (2) (1952) 387.

[13] T. Walter, R. Menner, C.H. Köble, H.W. Schock, Characterization and junction performance of highly efficient ZnO/CdS/$CuInS_2$ thin film solar cells, in: Proceedings of the 12th European Photovoltaic Solar Energy Conference and Exhibition, Amsterdam, The Netherlands, 1994, pp. 1755–1758.

[14] A.L. Fahrenbruch, R.H. Bube (Eds.), Fundamentals of Solar Cells, Academic Press, New York, 1983, p. 121f.

[15] M. El-Tahchi, A. Khoury, M. De Labardonnie, P. Mialhe, F. Pelanchon, Degradation of the diode ideality factor of silicon n–p junctions, Sol. Energy Mater. Sol. Cells 62 (2000) 393–398.

[16] K.R. Taretto, Modeling and characterization of polycrystalline silicon for solar cells and microelectronics, Ph.D. Thesis, Institut für Physikalische Elektronik—Universität Stuttgart, 2003, p. 25f.

[17] S.V. Karnik, M.K. Hatalis, Lateral polysilicon p^+–p–n^+ and p^+–n–n^+ diodes, Solid-State Electron. 47 (2003) 653–659.

[18] O. Breitenstein, J. Bauer, A. Lotnyk, J.M. Wagner, Defect induced non-ideal dark *I–V* characteristics of solar cells, Superlattice. Microstruct. 45 (2009) 182–189.

[19] M. Saad, A. Kassis, Effect of interface recombination on solar cell parameters, Sol. Energy Mater. Sol. Cells 79 (2003) 507–517.

[20] M. Saad, A. Kassis, Analysis of illumination-intensity-dependent *J–V* characteristics of ZnO/CdS/$CuGaSe_2$ single crystal solar cells, Sol. Energy Mater. Sol. Cells 77 (2003) 415–422.

[21] V. Nadenau, U. Rau, A. Jasenek, H.W. Schock, Electronic properties of $CuGaSe_2$-based heterojunction solar cells. Part I. Transport analysis, J. Appl. Phys. 87 (1) (2000) 584–594.

[22] M. Saad, A. Kassis, Thermally and light-activated current in ZnO/CdS/$CuGaSe_2$ single crystal solar cells, Renewable Energy 33 (2008) 974–978.

[23] H. Bayhan, A.S. Kavasoğlu, Tunnelling enhanced recombination in polycrystalline CdS/CdTe and CdS/Cu(In,Ga)Se_2 heterojunction solar cells, Solid-State Electron. 49 (2005) 991–996.

[24] H. Bayhan, Study of CdS/Cu(In,Ga)Se_2 interface by using n values extracted analytically from experimental data, Sol. Energy 83 (3) (2009) 372–376.

[25] H. Kobayashi, M. Takahashi, O. Maida, A. Asano, T. Kubota, J. Ivanc, A. Nakajima, K. Akimoto, Semiconductor surface and interface passivation by cyanide treatment, Appl. Surf. Sci. 235 (2004) 279–292.

[26] V. Schlosser, R. Ebner, J. Summhammer, P. Bajons, G. Klinger, LBIC Investigations of multicrystalline silicon solar cells with the front contact on grain boundaries, in: Proceedings of the 20th European Photovoltaic Solar Energy Conference and Exhibition, Barcelona, Spain, 2005, pp. 1135–1138.

[27] A. Virtuani, E. Lotter, M. Powalla, Performance of Cu(In,Ga)Se_2 solar cells under low irradiance, Thin Solid Films 431–432 (2003) 443–447.

[28] R.B. Bergmann, J.H. Werner, The future of crystalline silicon films on foreign substrates, Thin Solid Films 403–404 (2002) 162–169.